Transbilayer Peptide Sorting between Raft and Nonraft Bilayers: Comparisons of Detergent Extraction and Confocal Microscopy

Adriana Vidal and Thomas J. McIntosh
Department of Cell Biology, Duke University Medical Center, Durham, North Carolina 27710

ABSTRACT Membrane microdomains (''rafts'') that sequester specific proteins and lipids are often characterized by their resistance to detergent extraction. Because rafts are enriched in sphingomyelin and cholesterol, raft bilayers are thicker and have larger area compressibility moduli than nonraft bilayers. It has been postulated that rafts concentrate proteins with long transmembrane domains (TMDs) because of ''hydrophobic matching'' between the TMDs and the thick raft bilayers. However, previous detergent extraction experiments with bilayers containing raft and nonraft domains have shown that the peptides P-23 and P-29, designed to have single TMDs matching the hydrocarbon thicknesses of detergent soluble membranes and detergent resistant membranes, respectively, are both localized to detergent soluble membranes. Those results imply that both peptides are preferentially located in nonraft domains. However, because the detergent solubilizes part of the bilayer, it has been unclear whether or not detergent extraction experiments provide an accurate indication of the location of peptides in intact bilayers. Here we use confocal microscopy to examine the distribution of these same peptides in intact bilayers containing both raft and nonraft domains. At 20°C and 37°C, P-23 and P-29 were both primarily localized in fluorescently labeled nonraft domains. These confocal results validate the previous detergent extraction experiments and demonstrate the importance of bilayer cohesive properties, compared to hydrophobic mismatch, in the sorting of these peptides that contain a single TMD.

INTRODUCTION

Cell plasma and Golgi membranes are thought to contain small microdomains or ''rafts'' that are enriched in specific lipids and proteins (1,2). Due to their ability to sequester these membrane components, rafts have been shown to be involved in many key cellular functions, including signal transduction (3–7), membrane fusion (8–10), organization of the cytoskeleton (11,12), lipid sorting (13–15), protein trafficking (1,16–20), and localization and activity of specific membrane channels (21–23). Rafts have also been shown to exist in lipid bilayers containing lipid compositions approximating those of plasma membranes (24–27). In both natural and bilayer membranes, rafts have been characterized by their insolubility at low temperatures in detergents such as Triton X-100 (7,24,28–30), and it has been found that detergent resistant membranes (DRMs) are enriched in specific lipids, including sphingomyelin (SM) and cholesterol (1,15,31–33).

A fundamental question about membrane rafts concerns the mechanisms by which raft components are distributed in the plane of the membrane. Because of the similarity in composition of rafts in cell membranes and lipid bilayers, bilayer systems are currently being used to analyze the molecular interactions responsible for the sorting of lipids and proteins between raft and nonraft bilayers (34–37). In the sorting of transmembrane proteins, a recent theoretical analysis (38) considers two key factors in the differences between rafts and nonrafts: 1), bilayer thickness, and 2), bilayer material (cohesive or elastic) properties. DRMs extracted from lipid mixtures have hydrocarbon cores ~25% thicker than those of detergent soluble membranes (DSMs) (35), and the area compressibility modulus (K_a) of SM/cholesterol bilayers is ~7 times that of typical nonraft phosphatidylcholine (PC) bilayers (39–41).

Bilayer thickness is thought to be a factor in protein-lipid interactions because of the effects of ''hydrophobic matching'' between the bilayer hydrocarbon thickness and the length of the transmembrane domain (TMD) of the protein (42). That is, due to the energetic cost of exposing either hydrocarbon or hydrophobic amino acids to water, the most energetically favorable interaction between a bilayer and a transmembrane protein occurs when the bilayer hydrocarbon thickness matches the length of the protein TMD (38). The bilayer material properties are expected to be important in sorting transmembrane proteins for two main reasons. First, the incorporation of a protein into a bilayer requires the creation of volume by the separation of adjacent lipid molecules in the plane of the bilayer. For SM/cholesterol bilayers with large cohesive energies (large values of K_a), more energy is required to separate adjacent lipid molecules than for typical unsaturated PC bilayers (lower values of K_a) (43). It has recently been shown that the free energy of partitioning of specific water-soluble peptides into electrically neutral bilayers is a linear function of K_a (43,44). Second, theoretical treatments indicate that the energetic cost of bilayer deformation caused by hydrophobic mismatch between bilayer and protein TMD depends on bilayer elastic properties (38,45).

Recent experiments have been performed to test the role of hydrophobic mismatch in the sorting of transbilayer peptides

Submitted March 4, 2005, and accepted for publication May 16, 2005.

Address reprint requests to Thomas J. McIntosh, E-mail: t.mcintosh@cellbio.duke.edu.

0006-3495/05/08/1102/07 $2.00

doi: 10.1529/biophysj.105.062380

into or out of bilayer rafts (34,35). These experiments used sets of peptides with single bilayer spanning regions with TMD lengths matching the measured hydrocarbon thicknesses of DRM bilayers or DSM bilayers (Fig. 1). Detergent extraction experiments indicated that, independent of peptide length, transbilayer peptides were enriched in DSMs compared to DRMs (34,35). However, one potential problem with these previous experiments is their reliance on detergent extraction to determine the localization of the transmembrane peptides in raft or nonraft bilayers. In addition to breaking up the bilayer, it has been shown that Triton may create ordered domains in homogeneous fluid bilayers (30). Therefore, one wonders whether the detergent extraction procedure provides an accurate picture of the localization of the peptides in intact bilayers containing both raft and nonraft bilayer microdomains (35).

In this study, we use confocal microscopy with fluorescently labeled lipids and peptides to determine the distribution of transbilayer peptides in intact giant unilamellar vesicles (GUVs) composed of 1:1:1 dioleoylphosphatidylcholine (DOPC)/SM/cholesterol, a well-characterized lipid system, that has been shown to contain both raft and nonraft bilayers (25,27,46–48). We examined the GUVs at two temperatures, room temperature (20°C) and physiological temperature (37°C), since there appears to be a phase transition in this system near physiological temperature (27). Comparisons of data from detergent extraction (34,35) and these confocal experiments with intact bilayers should provide information on 1) the effects of detergent on raft organization, and 2) the relative importance of bilayer thickness and cohesive properties on the in-plane sorting of peptides with single TMDs.

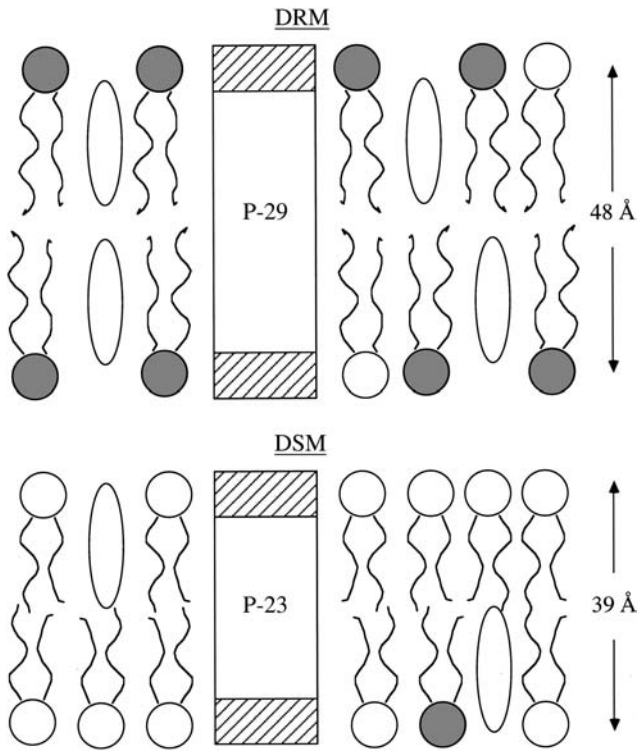

FIGURE 1 Schematic drawing showing peptides P-29 ($KKG(LA)_5LW(LA)_5LKKA$) and P-23 ($KKG(LA)_4W(LA)_4KKA$) where the lengths of the hydrophobic α-helices were designed to closely match the hydrocarbon thicknesses obtained from x-ray diffraction (35) of DRMs and DSMs from 1:1:1 DOPC/SM/cholesterol bilayers. For each peptide, the white central box corresponds to the transbilayer region and the hatched boxes correspond to the hydrophilic regions. Cholesterol molecules are drawn as open ovals, and phospholipids are depicted with wavy hydrocarbon chains and circular headgroups (*shaded* headgroups represent SM and *open* headgroups represent DOPC). Van Duyl et al. (34) used similar peptides with tryptophans rather than lysines in the hydrophilic regions. This figure, redrawn from McIntosh et al. (35), was used with permission.

MATERIALS AND METHODS

Materials

Brain SM, DOPC, and cholesterol were purchased from Avanti Polar Lipids (Alabastar, AL). Cholesterol infinity reagent, Triton X-100, Sephadex G-50, and Hepes were purchased from Sigma Chemical (St. Louis, MO). The CBQCA Protein Quantification Kit and the fluorescent lipid probe 3,3′-dilinoleoyloxacarbocyanine perchlorate (DiO-C18:2) were obtained from Molecular Probes (Eugene, OR).

The vesicles used in our studies contained 1:1:1 DOPC/SM/cholesterol because this (or similar mixtures of these lipids) forms bilayers containing rafts and nonrafts (25,27,46–48), and the composition and bilayer thickness have been obtained for DRMs and DSMs (33). The two peptides used were P-23 ($KKG(LA)_4W(LA)_4KKA$), which contained 23 amino acids with a central hydrophobic stretch of 17 amino acids, and P-29 ($KKG(LA)_5LW(LA)_5LKKA$), which contained 29 amino acids with a central hydrophobic region of 23 amino acids (Fig. 1). P-23 and P-29 were chosen since their hydrophobic lengths match the hydrocarbon thickness of DSMs and DRMs, respectively, of the DOPC/SM/cholesterol system (35). The peptides were synthesized and purified by the Micro Protein Chemistry Facility at the University of North Carolina (Chapel Hill, NC) as described previously (35). For confocal microscopy experiments some of the P-23 and P-29 peptides had rhodamine conjugated to the amino terminus of each peptide using the 5-TAMRA-OH reagent (Biosearch Technologies, Novato, CA) solubilized in dimethylformamide (5 mg/ml) along with 10 mg of 1-hydoxy-7-azabenzotriazole. That solution was activated by the addition of 10 μl of diisopropylcarbodiimide for 2 min and then added for an overnight reaction to the previously dried peptide-containing resin. The resin was washed with dimethylformamide, and the peptide was cleaved from the resin and deprotected in the usual fashion.

Methods

Detergent extractions at 20°C used standard procedures as described in detail previously (33). In brief, peptide/lipid mixtures (1 mg peptide/10 mg total lipid) were codissolved in chloroform/methanol, rotary evaporated to dryness, hydrated, treated with 1% Triton X-100 for 30 min, and then centrifuged. The phospholipid, cholesterol, and peptide contents of the supernatant (DSMs) and resuspended pellet (DRMs) were determined as described previously (35).

For confocal microscopy experiments, GUVs on the order of 20–40 μm in diameter were made by the procedures of Akashi et al. (49) with slight modifications. The same lipid-peptide mixtures used for the detergent extraction experiments were used in the confocal experiments, except that the lipids contained 0.1% DiO-C18:2 and the peptides included 4% rhodamine-labeled peptide. The lipid-peptide was dissolved in chloroform/methanol, evaporated on a Teflon plate under vacuum for 3 h, covered with

0.1 M sucrose in distilled water (internal medium), and incubated over night at 37°C. The resulting ''lipid cloud'' that detached from the Teflon was collected in plastic tubes and prepared for the microscope observation by diluting with 0.1 M glucose in distilled water (external solution), placing on a microscope slide, and covering with a glass coverslip. Since the inside of the vesicles contained sucrose and the outside contained the lower density glucose, the GUVs sank to the microscope slide.

The GUVs were observed with a 63× NA 1.4 Plan Apochromat oil objective on a LSM 510 Meta Zeiss Confocal Microscope (Jena, Germany). Configurations for double channel excitation and the choice of emission of the fluorochromes were made to prevent cross talk, and the two colors were scanned simultaneously. The green DiO lipid labels were observed with the use of a 488 nm filter, whereas the rhodamine-labeled peptides were observed with a 543 nm filter. Specimen temperature was controlled using a Zeiss P-insert LabTek stage, and the temperature at the sample was verified with a small thermocouple. Quantification of lipid and peptide probe colocalization was performed with the Zeiss LSM AIM 3.2 Enhanced Colocalization software. This software gives overlap coefficients between 0.0 and 1.0, with 1.0 representing the maximum overlap of the two probes. This overlap coefficient gives a measure of the colocalization of lipid and peptide probes, independent of their localization in raft or nonraft bilayer.

RESULTS

The 1:1:1 DOPC/SM/cholesterol dispersions were fractionated into a supernatant (DSMs) and pellet (DRMs) by treatment with 1% Triton X-100 at 20°C. Most of the peptide, either P-23 or P-29, was located in the DSMs. That is, when normalized to the total lipid (phospholipid plus cholesterol) in each domain, the molar ratio of peptide in the DSMs to the DRMs was 6.0 and 5.5 for P-23 and P-29, respectively. Previously, we (35) found that the comparable molar ratios of peptides in DSMs to DRMs were 9.8 for P-23 and 6.2 for P-29 at 4°C and 3.9 for P-23 and 1.7 for P-29 at 37°C. Thus, for either P-23 or P-29, at all temperatures tested more peptide was found in DSMs than in DRMs, and the results at 20°C were between those obtained at 4°C and 37°C.

GUVs were made containing rhodamine-labeled peptide and the green fluorescent lipid DiO-C18:2, which contains two unsaturated hydrocarbon chains. DiO-C18:2 has been shown to partition preferentially into liquid-disordered, nonraft bilayers (50).

Fig. 2 shows confocal images recorded at 20°C of three DOPC/SM/cholesterol GUVs containing the green DiO-C 18:2 and the red rhodamine-labeled P-23. In the left-hand column, intensely green-labeled microdomains contrasted with unlabeled or lightly labeled microdomains. The intensely labeled regions were identified as nonraft bilayer since the ratio of labeled to unlabeled bilayer increased when the ratio of DOPC to cholesterol was increased (data not shown). As seen in the middle and right-hand columns, the same microdomains that preferentially contained DiO also contained the P-23 label. There was a strong colocalization of the peptide with the DiO-C18:2, as the labeled peptide-labeled lipid (*red-green*) overlap value was 0.9 for P-23.

Confocal images of equimolar DOPC/SM/cholesterol GUVs at 20°C labeled with DiO-C18:2 and P-29 are shown in Fig. 3. For P-29, there was also a strong colocalization of the peptide with the DiO-C18:2 as seen in the middle and right-hand columns. The labeled peptide-labeled lipid (*red-green*) overlap value was 0.9 for P-29. On average, the

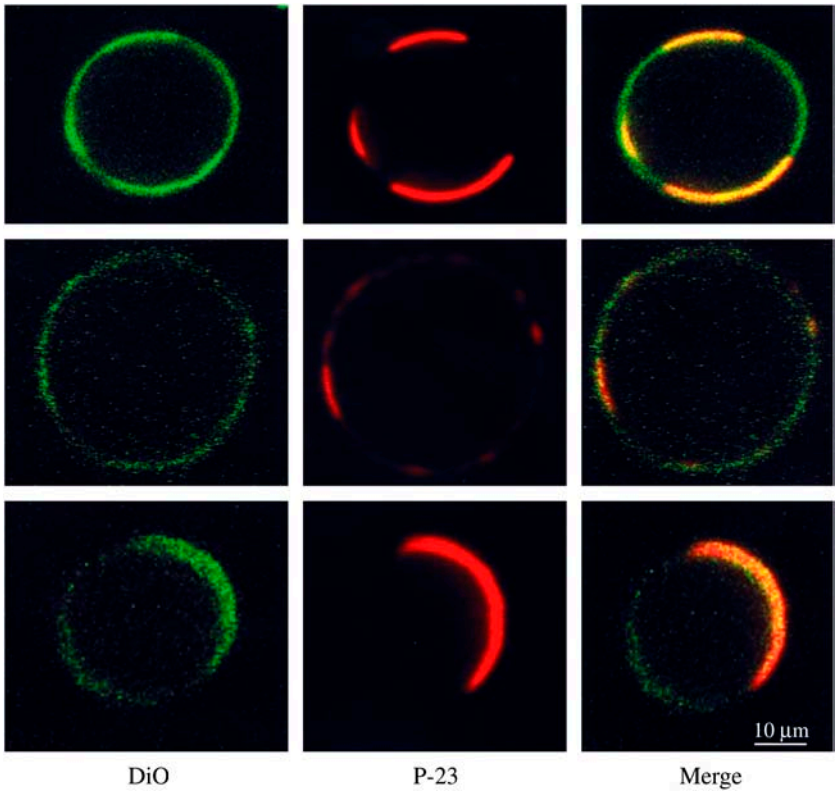

FIGURE 2 Confocal images of 1:1:1 DOPC/SM/cholesterol containing rhodamine-labeled P-23 and the lipid DiO-C18:2. The left column shows the green fluorescent lipid label DiO, the middle column shows the rhodamine-labeled P-23, and the right column is a color-merged image. The three rows show three different vesicles from the same preparation. All images were taken at 20°C at the same magnification.

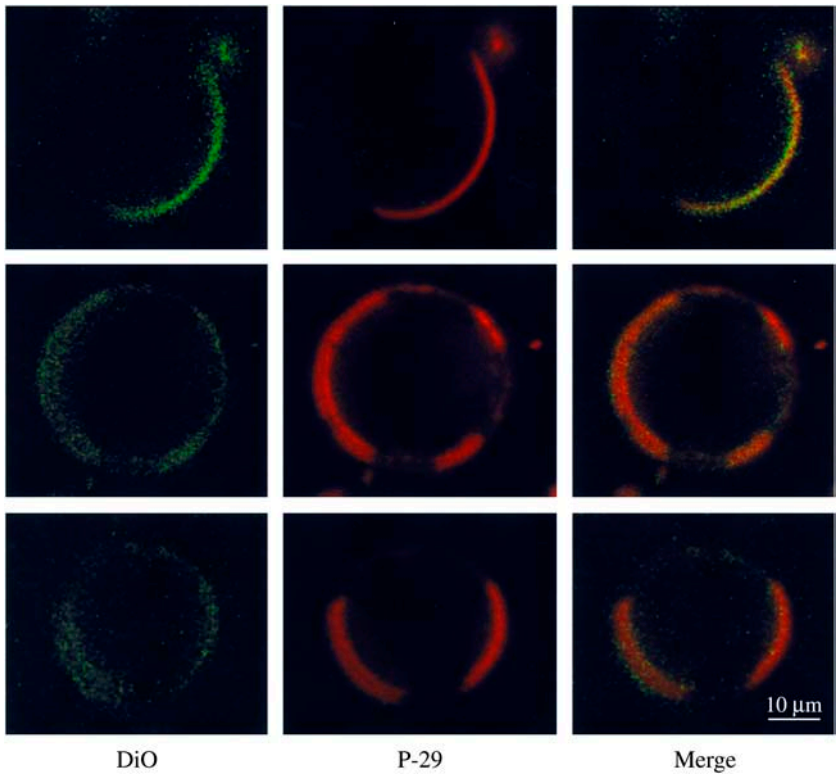

FIGURE 3 Confocal images of 1:1:1 DOPC/SM/cholesterol GUVs containing rhodamine-labeled P-29 and DiO-C18:2. The left column is the fluorescence image showing the DiO lipid label, the middle column shows the rhodamine-labeled P-29, and the right column is a color-merged image. The three rows show three different vesicles from the same preparation. All images were taken at 20°C at the same magnification.

DiO-C18:2 appeared to label <½ of the equator in the presence of either P-23 (Fig. 3) or P-29 (Fig. 4). In some instances, such as the bottom row in Fig. 2 or the top row in Fig. 3, the equator contained one large labeled domain. In other cases, such as the top row of Fig. 2 or the bottom two rows of Fig. 3, two or more smaller labeled domains were seen in each vesicle.

Confocal experiments were also performed for equimolar DOPC/SM/cholesterol GUVs at physiological temperature (37°C). Although many GUVs did not display microdomains (not shown), we observed clear microdomain organization in several vesicles, such as the one shown in Fig. 4. In GUVs that did display microdomains, the labeled nonraft domain took up a larger fraction of the equator at 37°C (Fig. 4) than at 20°C (Fig. 3). Although the size and location of the labeled domains changed as a function of incubation time, at all times there was a strong colocalization of DiO-C18:2 and P-29 (Fig. 4), as the labeled peptide-labeled lipid overlap was 0.8 to 0.9. Microdomains were visible for a least 1 h incubation at 37°C. When the temperature was cooled back to 20°C (data not shown) there was microdomain reorganization such that almost all vesicles again displayed microdomains as they did before the temperature was increased to 37°C (Fig. 4).

DISCUSSION

Previously, we (35) have shown that a large fraction of the transbilayer peptides P-23 and P-29 are detergent extracted from lipid vesicles composed of DOPC/SM/cholesterol at either 4°C (the temperature at which many detergent extractions are performed) or 37°C. That is, independent of the peptide length, both of these peptides are enriched in DSMs. Van Duyl et al. (34) obtained similar results with similar sets of transbilayer peptides at 4°C. Quantitative analysis of the concentration of lipid and peptide in DSMs and DRMs allowed us to calculate partition coefficients and apparent free energies of transfer of the peptides from DSMs to DRMs (35). However, a potential problem with that analysis is that the detergent breaks up the bilayer and thus might affect the distribution of peptides and lipids. Here we examined the distribution of these peptides in intact GUVs by the use of confocal microscopy.

Because confocal microscopy was more readily performed at 20°C than at 4°C, we determined here the distribution by detergent extraction of P-23 and P-29 in DRMs and DSMs at 20°C. We found similar distributions of both peptides at 4°C and 20°C.

The unsaturated lipid probe DiO-C18:2 clearly demarcated nonraft domains, as vesicles containing this probe always contained both heavily labeled and nearly unlabeled regions around the vesicles' equators (Figs. 2–4). At 20°C both P-23 (Fig. 2) and P-29 (Fig. 3) were highly colocalized with DiO-C18:2. Since DiO-C18:2 is primarily localized in nonraft (liquid-crystalline) regions of GUVs (50), this indicates that both peptides preferentially partitioned into the nonraft domains of the vesicle.

Although we did not observe rafts in all vesicles at 37°C, microdomains were clearly visible in some GUVs (Fig. 4).

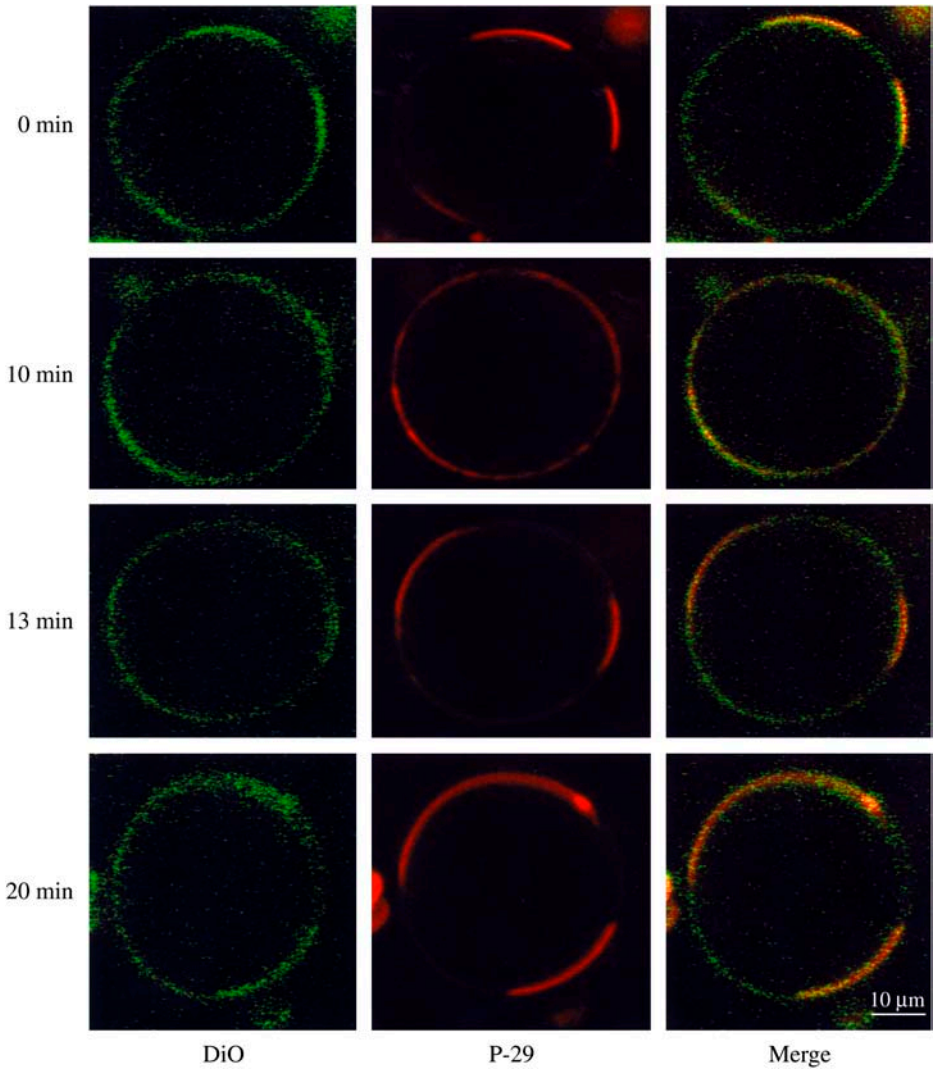

FIGURE 4 Confocal images of 1:1:1 DOPC/SM/cholesterol containing rhodamine-labeled P-29 and DiO-C18:2 taken at 37°C. The left column is the fluorescence image showing the DiO lipid label, the middle column shows the rhodamine-labeled P-29, and the right column is a color-merged image. The four rows show the same vesicle imaged with increasing incubation times at 37°C, as noted on the left-hand side of the figure.

At 37°C, P-29 and DiO-C18:2 were colocalized (Fig. 4), indicating the preference of P-29 for nonraft domains at this temperature. The labeled nonraft domains occupied a larger fraction of the equator at 37°C than at 20°C (Fig. 3). As a function of time, the labeled nonraft domains changed size and location on the equator of these GUVs, indicating the transient nature of these microdomains. These observed transient changes could be either due to movement of entire microdomains or the movement of individual lipid or peptide molecules into or out of the domains. These observations on the temperature dependence of domain formation can be compared to previous studies of DOPC/SM/cholesterol bilayers containing fluorescently labeled lipids that showed as the temperature was raised unlabeled lipid rafts became smaller until they were nonresolvable with the light microscope at 37°C (25,27,46). Possible reasons for differences among these observations are variability in the hydrocarbon chain composition of the natural brain SM and possible small variability in lipid composition from one GUV to another. Veatch and Keller (46) found that the miscibility temperature depends on the SM chain composition and the phospholipid/cholesterol ratio. Moreover, in our experiments the nonraft microdomains were more clearly demonstrated with the labeled P-29 (*middle column* Fig. 4) than with the DiO lipid label (*left-hand column* of Fig. 4).

The confocal experiments on intact vesicles are consistent with our detergent extraction data (35) in several ways. First, the confocal experiments show the presence of microdomains at both 20°C and 37°C, consistent with the observations that there are detergent soluble and detergent insoluble fractions at these temperatures. Second, the fraction of labeled nonraft domain increased with increasing temperature (Figs. 3 and 4), as did the amount of detergent soluble lipid (35). Third, both transbilayer peptides P-23 and P-29 were preferentially localized in nonraft bilayers (Figs. 2–4) and a large fraction of these peptides were extracted in DSMs (35). However, by detergent extraction we (35) found that somewhat more P-29 than P-23 was found in DRMs. This difference was not detectable by confocal microscopy.

Importantly, the confocal and detergent extraction experiments provide complementary data on the sorting of transmembrane peptides. The confocal experiments give direct information for the preference of both P-23 and P-29 for nonraft bilayers in intact vesicles. However, these confocal data are relatively nonquantitative and are limited by sampling problems inherent to most microscopic techniques. In contrast, the detergent extraction experiments, coupled with biochemical analyses, provide quantitative data on the distribution of the lipid and peptide components for large quantities (milligrams) of sample.

Thus, many of the observations on the sorting of peptides P-23 and P-29 obtained with detergent extraction experiments were verified by confocal observations of intact vesicles. Importantly, both P-23 and P-29 were preferentially localized in nonraft bilayers. Since the TMD of P-23 matched the width of the nonraft bilayer, whereas the TMD of P-29 matched the width of the raft bilayer (Fig. 1), it appears that hydrophobic matching is not the primary factor in sorting these peptides in the plane of the bilayer. Rather, in agreement with previous analyses (34,35,38,51), we argue that the difference in lipid cohesive (packing) properties between raft (enriched in SM/cholesterol) and nonraft bilayers (enriched in DOPC) is an important factor in the preference of peptides with single TMDs for nonraft bilayers. That is, the relatively low area compressibility modulus of DOPC bilayers compared to SM/cholesterol bilayers (39,41) makes it energetically favorable for these transbilayer peptides to partition into nonraft bilayers. For membrane proteins other factors are also in play, such as specific amino acid sequences in the TMDs (52) and cytosolic domains (53).

We thank Dr. Tim Oliver for his expert assistance with the confocal experiments.

This work was supported by National Institutes of Health Grant GM27278.

REFERENCES

1. Simons, K., and E. Ikonen. 1997. Functional rafts in cell membranes. *Nature*. 387:569–572.
2. Gkantiragas, I., B. Brugger, E. Stuven, D. Kaloyanova, X.-Y. Li, K. Lohr, F. Lottspeich, F. T. Wieland, and J. B. Helms. 2001. Sphingomyelin-enriched microdomains at the Golgi complex. *Mol. Biol. Cell*. 12:1819–1833.
3. Field, K. A., D. Holowka, and B. Baird. 1997. Compartmentalized activation of the high affinity immunoglobulin E receptor within membrane domains. *J. Biol. Chem.* 272:4276–4280.
4. Baird, B., E. D. Sheets, and D. Holowka. 1999. How does the plasma membrane participate in cellular signaling by receptors for immunoglobulin E? *Biophys. Chem.* 82:109–119.
5. Kawabuchi, M., Y. Satomi, T. Takao, Y. Shimonishi, S. Nada, K. Nagai, A. Tarakhovsky, and M. Okada. 2000. Transmembrane phosphoprotein Chp regulates the activity of Src-family of tyrosine kinase. *Nature*. 404:999–1003.
6. Moffett, S., D. A. Brown, and M. E. Linder. 2000. Lipid-dependent targeting of G proteins into rafts. *J. Biol. Chem.* 275:2191–2198.
7. Simons, K., and D. Toomre. 2000. Lipid rafts and signal transduction. *Nat. Rev. Mol. Cell Biol.* 1:31–39.
8. Lang, T., D. Bruns, D. Wenzel, D. Riedel, P. Holroyd, C. Thiele, and R. Jahn. 2001. SNAREs are concentrated in cholesterol-dependent clusters that define docking and fusion sites for exocytosis. *EMBO J.* 20:2202–2213.
9. Chamberlain, L. H., R. D. Burgoyne, and G. W. Gould. 2001. SNARE proteins are highly enriched in lipid rafts in PC12 cells: implications for the spatial control of exocytosis. *Proc. Natl. Acad. Sci. USA*. 98:5619–5624.
10. Chamberlain, L. H., and G. W. Gould. 2002. The vesicle- and target-SNARE proteins that mediate Glut4 vesicle fusion are localized in detergent-insoluble lipid rafts present on distinct intracellular membranes. *J. Biol. Chem.* 277:49750–49754.
11. Laux, T., K. Fukami, M. Thelen, T. Golub, D. Frey, and P. Caroni. 2000. GAP43, MARCKS, and CAP23 modulate PI(4,5)P(2) at plasmalemmal rafts, and regulate cell cortex actin dynamics through a common mechanism. *J. Cell Biol.* 149:1455–1472.
12. Caroni, P. 2001. New EMBO members' review: actin cytoskeleton regulation through modulation of PI(4,5)P(2) rafts. *EMBO J.* 20:4332–4336.
13. Simons, K., and G. van Meer. 1988. Lipid sorting in epithelial cells. *Biochemistry.* 27:6197–6202.
14. Brown, D. A., and E. London. 1998. Functions of lipid rafts in biological membranes. *Annu. Rev. Cell Dev. Biol.* 14:111–136.
15. Simons, K., and E. Ikonen. 2000. How cells handle cholesterol. *Science*. 290:1721–1726.
16. Lafont, F., P. Verkade, T. Galli, C. Wimmer, D. Louvard, and K. Simons. 1999. Raft association of SNAP receptors acting in apical trafficking in Madin-Darby canine kidney cells. *Proc. Natl. Acad. Sci. USA*. 96:3734–3738.
17. Ikonen, E. 2001. Roles of lipid rafts in membrane transport. *Curr. Opin. Cell Biol.* 13:470–477.
18. Keller, P., D. Toomre, E. Diaz, J. White, and K. Simons. 2001. Multicolour imaging of post-Golgi sorting and trafficking in live cells. *Nat. Cell Biol.* 3:140–150.
19. Helms, J. B., and C. Zurzolo. 2004. Lipids as targeting signals: lipid rafts and intracellular trafficking. *Traffic*. 5:247–254.
20. Polishchuk, R., A. Di Pentima, and J. Lippincott-Schwartz. 2004. Delivery of raft-associated, GPI-anchored proteins to the apical surface of polarized MDCK cells by a transcytotic pathway. *Nat. Cell Biol.* 6:297–307.
21. Schubert, A. L., W. Schubert, D. C. Spray, and M. P. Lisanti. 2002. Connexin family members target to lipid raft domains and interact with caveolin-1. *Biochemistry*. 41:5754–5764.
22. Martens, J. R., K. O'Connell, and M. Tamkun. 2004. Targeting of ion channels to membrane microdomains: localization of KV channels to lipid rafts. *Trends Pharmacol. Sci.* 25:16–21.
23. Wong, W., and L. C. Schlichter. 2004. Differential recruitment of Kv1.4 and Kv4.2 to lipid rafts by PSD-95. *J. Biol. Chem.* 279: 444–452.
24. Ahmed, S. N., D. A. Brown, and E. London. 1997. On the origin of sphingolipid/cholesterol-rich detergent-insoluble cell membranes: physiological concentrations of cholesterol and sphingolipid induced formation of a detergent-insoluble, liquid-ordered lipid phase in model membranes. *Biochemistry*. 36:10944–10953.
25. Dietrich, C., L. A. Bagatolli, Z. N. Volovyk, N. L. Thompson, M. Levi, K. Jacobson, and E. Gratton. 2001. Lipid rafts reconstituted in model membranes. *Biophys. J.* 80:1417–1428.
26. Rinia, H. A., and B. deKruijff. 2001. Imaging domains in model membranes with atomic force microscopy. *FEBS Lett.* 504:194–199.
27. Samsonov, A. V., I. Mihalyov, and F. S. Cohen. 2001. Characterization of cholesterol-sphingomyelin domains and their dynamics in bilayer membranes. *Biophys. J.* 81:1486–1500.
28. Hanada, K., M. Nishijima, Y. Akamatsu, and R. E. Pagano. 1995. Both sphingolipids and cholesterol participate in the detergent insolubility of

alkaline-phosphatase, a glycosylphosphatidylinositol-anchored protein, in mammalian membranes. *J. Biol. Chem.* 270:6254–6260.

29. London, E., and D. A. Brown. 2000. Insolubility of lipids in Triton X-100: physical origin and relationship to spingolipid/cholesterol membrane domains (rafts). *Biochim. Biophys. Acta.* 1508:182–195.
30. Heerklotz, H. 2002. Triton promotes domain formation in lipid raft mixtures. *Biophys. J.* 83:2693–2701.
31. Brown, R. E. 1998. Sphingolipid organization in biomembranes: what physical studies of model membranes reveal. *J. Cell Sci.* 111:1–9.
32. Brown, D. A., and E. London. 2000. Structure and function of sphingolipid- and cholesterol-rich membrane rafts. *J. Biol. Chem.* 275:17221–17224.
33. Gandhavadi, M., D. Allende, A. Vidal, S. A. Simon, and T. J. McIntosh. 2002. Structure, composition, and peptide binding properties of detergent soluble bilayers and detergent resistant rafts. *Biophys. J.* 82:1469–1482.
34. van Duyl, B. Y., D. T. Rijkers, B. de Kruijff, and J. A. Killian. 2002. Influence of hydrophobic mismatch and palmitoylation on the association of transmembrane alpha-helical peptides with detergent-resistant membranes. *FEBS Lett.* 523:79–84.
35. McIntosh, T. J., A. Vidal, and S. A. Simon. 2003. Sorting of lipids and transmembrane peptides between detergent-soluble bilayers and detergent-resistant rafts. *Biophys. J.* 85:1656–1666.
36. Silvius, J. R. 2003. Role of cholesterol in lipid raft formation: lessons from lipid model systems. *Biochim. Biophys. Acta.* 1610:174–183.
37. Silvius, J. R. 2003. Fluorescence energy transfer reveals microdomain formation at physiological temperatures in lipid mixtures modeling the outer leaflet of the plasma membrane. *Biophys. J.* 85:1034–1045.
38. Lundbaek, J. A., O. S. Andersen, T. Werge, and C. Nielsen. 2003. Cholesterol-induced protein sorting: an analysis of energetic feasibility. *Biophys. J.* 84:2080–2089.
39. Needham, D., and R. S. Nunn. 1990. Elastic deformation and failure of lipid bilayer membranes containing cholesterol. *Biophys. J.* 58: 997–1009.
40. McIntosh, T. J., S. A. Simon, D. Needham, and C.-h. Huang. 1992. Structure and cohesive properties of sphingomyelin:cholesterol bilayers. *Biochemistry.* 31:2012–2020.
41. Rawicz, W., K. C. Olbrich, T. McIntosh, D. Needham, and E. Evans. 2000. Effect of chain length and unsaturation on elasticity of lipid bilayers. *Biophys. J.* 79:328–339.
42. Mouritsen, O. G., and M. Bloom. 1984. Mattress model of lipid-protein interactions in membranes. *Biophys. J.* 46:141–153.
43. Allende, D., A. Vidal, S. A. Simon, and T. J. McIntosh. 2003. Bilayer interfacial properties modulate the binding of amphipathic peptides. *Chem. Phys. Lipids.* 122:65–76.
44. Allende, D., S. A. Simon, and T. J. McIntosh. 2005. Melittin-induced bilayer leakage depends on lipid material properties: evidence for toroidal pores. *Biophys. J.* 88:1828–1837.
45. Nielsen, C., M. Goulian, and O. S. Andersen. 1998. Energetics of inclusion-induced bilayer deformations. *Biophys. J.* 74:1966–1983.
46. Veatch, S. L., and S. L. Keller. 2003. Separation of liquid phases in giant vesicles of ternary mixtures of phospholipids and cholesterol. *Biophys. J.* 85:3074–3083.
47. Veatch, S. L., I. V. Polozov, K. Gawrisch, and S. L. Keller. 2004. Liquid domains in vesicles investigated by NMR and fluorescence microscopy. *Biophys. J.* 86:2910–2922.
48. Veatch, S. L., and S. L. Keller. 2003. A closer look at the canonical ''raft mixture'' in model membrane systems. *Biophys. J.* 84:725–726.
49. Akashi, K.-I., H. Miyata, H. Itoh, and K. Kinosita. 1996. Preparation of giant liposomes in physiological conditions and their characterization under an optical microscope. *Biophys. J.* 71:3242–3250.
50. Feigenson, G. W., and J. T. Buboltz. 2001. Ternary phase diagram of dipalmitoyl-PC/Dilauroy-PC/cholesterol: nanoscopic domain formation driven by cholesterol. *Biophys. J.* 80:2775–2788.
51. Allende, D., A. Vidal, and T. J. McIntosh. 2004. Jumping to rafts: gatekeeper role of bilayer elasticity. *Trends Biochem. Sci.* 29: 325–330.
52. Scheiffele, P., M. G. Roth, and K. Simons. 1997. Interaction of influenza virus haemagglutinin with sphingolipid-cholesterol membrane domains via its transmembrane domain. *EMBO J.* 16:5501–5508.
53. Crossthwaite, A. J., T. Seebacherm, N. Massada, A. Ciruela, K. Dufraux, J. E. Schultz, and D. M. F. Cooper. 2005. The cytosolic domains of Ca2+-sensitive adenylyl cyclases dictate their targeting to plasma membrane lipid rafts. *J. Biol. Chem.* 280:6380–6391.